Single-Cell RNA Sequencing Reveals Multiple Pathways and the Tumor Microenvironment Could Lead to Chemotherapy Resistance in Cervical Cancer

Meijia Gu [1], Ti He [2], Yuncong Yuan [3,4], Suling Duan [1], Xin Li [5*] and Chao Shen [3,4*]

[1] Key Laboratory of Combinatorial Biosynthesis and Drug Discovery, Ministry of Education, School of Pharmaceutical Sciences, Wuhan University, Wuhan, China, [2] Department of Scientific Research & Industrial Application, Beijing Microread Genetics Co., Ltd., Beijing, China, [3] College of Life Sciences, Wuhan University, Wuhan, China, [4] China Center for Type Culture Collection, Wuhan University, Wuhan, China, [5] Department of Gynecology 2, Renmin Hospital of Wuhan University, Wuhan, China

Background: Cervical cancer is one of the most common gynecological cancers worldwide. The tumor microenvironment significantly influences the therapeutic response and clinical outcome. However, the complex tumor microenvironment of cervical cancer and the molecular mechanisms underlying chemotherapy resistance are not well studied. This study aimed to comprehensively analyze cells from pretreated and chemoresistant cervical cancer tissues to generate a molecular census of cell populations.

Methods: Biopsy tissues collected from patients with cervical squamous cell carcinoma, cervical adenocarcinoma, and chronic cervicitis were subjected to single-cell RNA sequencing using the 10× Genomics platform. Unsupervised clustering analysis of cells was performed to identify the main cell types, and important cell clusters were reclustered into subpopulations. Gene expression profiles and functional enrichment analysis were used to explore gene expression and functional differences between cell subpopulations in cervicitis and cervical cancer samples and between chemoresistant and chemosensitive samples.

Results: A total of 24,371 cells were clustered into nine separate cell types, including immune and non-immune cells. Differentially expressed genes between chemoresistant and chemosensitive patients enriched in the phosphoinositide 3-kinase (PI3K)/AKT pathway were involved in tumor development, progression, and apoptosis, which might lead to chemotherapy resistance.

Conclusions: Our study provides a comprehensive overview of the cancer microenvironment landscape and characterizes its gene expression and functional difference in chemotherapy resistance. Consequently, our study deepens the insights into cervical cancer biology through the identification of gene markers for diagnosis, prognosis, and therapy.

Keywords: single-cell RNA sequencing, cervical cancer, tumor microenvironment, chemotherapy resistance, multiple pathways

INTRODUCTION

As the fourth most common gynecological malignant tumor, cervical cancer is a leading cause of cancer-related deaths among women and poses a serious threat to the health of women worldwide (1). In 2018, approximately 570,000 new cases of cervical cancer and 311,000 deaths from this cancer were reported (1). Paclitaxel, cisplatin, carboplatin, or a combination of these agents is the front-line treatment for cervical cancer (2). However, the efficacy of current chemotherapeutic agents is limited, with relatively low response rates of 29%–63% because of chemotherapy resistance (3). The combination of paclitaxel and cisplatin is one of the most commonly utilized regimens in the metastatic disease setting (4). However, in actual clinical treatment, tumor cells often develop resistance.

The tumor microenvironment (TME) comprises various cell types [such as fibroblasts, endothelial cells (ECs), and immune cells] and extracellular components (such as cytokines, hormones, extracellular matrix, and growth factors), which surround tumor cells as a vascular network. The TME not only plays a pivotal role during tumor initiation, progression, and metastasis, but it also has profound effects on therapeutic efficacy. TME-mediated chemotherapy resistance is a result of complex crosstalk between tumor cells and their surrounding environment (5, 6).

For example, the TME and therapeutic response can be induced by soluble factors secreted by tumors. The adhesion of tumor cells to stromal fibroblasts can also affect responses to chemotherapy (7), and immune cells also play an important role in improving and obstructing therapeutic efficacy (7). The interaction between chemotherapy sensitivity and TME is a complex phenomenon. Cancers can develop remarkable resistance to various treatments that target different molecular pathways (8).

Research studies have shown that the cellular and molecular mechanisms underlying the development of resistance are multifactorial and include genetic and epigenetic alterations, cell detoxification, and abnormal drug efflux and accumulation (9, 10). However, the molecular mechanisms underlying the occurrence and development of resistance are poorly understood. Thus, there is an urgent need to identify the basic factors that determine chemotherapy resistance in cancer.

Previous studies on molecular mechanisms and chemotherapy resistance in cervical cancer patients have focused mainly on bulk genomic or transcriptome profiling

methods and *in-situ* hybridization techniques (11–13). Consequently, studies of chemoresistance mechanisms based on the signatures of distinct cell populations are obscure (10–12). Single-cell RNA sequencing (scRNA-seq) techniques have emerged as a powerful tool for analyzing the spectrum of cell populations in tissues. Furthermore, these techniques have been widely used for elucidating the complex subpopulations in tissues of organs such as the lung (14), heart (15), and brain (16), as well as in various cancers including melanoma (17), ovarian (18), and colon (19) cancers (20, 21).

Although studies have used scRNA-seq on the cervix uteri (22) and drug-resistant cell lines (12), to the best of our knowledge, scRNA-seq profiling of human cervical cancer tissues has not been reported to date. Although scRNA-seq is increasingly being adopted, its application to tumors has been limited to several types, but not cervical cancer. Because of this limited elucidation of human tumors and the lack of TME profiling, the intratumoral transcriptomic heterogeneity of the most common cancer in women is largely unknown.

Exploring the molecular mechanism of chemotherapy resistance is important in the development of strategies to overcome tumor resistance and provides a theoretical basis for reversing tumor resistance and improving cancer chemotherapy efficacy. The development of chemotherapy combinations that could simultaneously target tumor cells and the microenvironment may represent a solution to overcome chemotherapy resistance. This study aimed to analyze cells from pretreated and chemoresistant cervical cancer tissues at a much higher scale, to generate a molecular census of cell populations.

Furthermore, we sought to uncover the cell heterogeneity using unbiased scRNA-seq techniques. Consequently, we performed an scRNA-seq survey of 23,444 cells from five tissues from pretreated cervical cancer patients and constructed a single-cell transcriptome atlas for early malignancy of cervical cancer (**Figure 1**). Our study provides novel insights into the heterogeneity of cervical cancer at the single-cell level and will serve as a valuable resource for understanding chemotherapy resistance mechanisms in tumor progression.

MATERIALS AND METHODS

Patients and Tumor Specimens

Four female patients with a pathologic diagnosis of cervical cancer and one female patient diagnosed with cervicitis were enrolled at Renmin Hospital of Wuhan University, Wuhan (**Table 1**). All enrolled patients signed the written consent, and this study was approved by the Institutional Review Board (IRB) of Renmin Hospital of Wuhan University (IRB no. WDRY2021-K014). Fresh tumor samples (at least 1.5 cm^3) were surgically resected from all enrolled patients. None of the patients were treated with chemotherapy prior to tissue sample collection. After sample resection, three of the four cervical cancer patients were treated with chemotherapy, and one patient was a responder and the two were resistant to chemotherapy.

Abbreviations: CBP, carboplatin; CA, cervical adenocarcinoma; CE, chronic cervicitis; CQ, cervical squamous cell carcinoma; DEGs, differentially expressed genes; ECs, endothelial cells; FAP, fibroblast activating protein; FDR, false discovery rate; GO, Gene Ontology; HGF, hepatocyte growth factor; KEGG, Kyoto Encyclopedia of Genes and Genomes; PCA, principal component analysis; PDL1, programmed cell death ligand 1; PDL2, programmed cell death ligand 2; PLD1, phospholipase D1; PLVAP, plasmalemmal vesicle-associated protein; scRNA-seq, single-cell RNA sequencing; SDF1, stromal cell-derived factor 1; *t*-SNE, t-distributed stochastic neighbor embedding; TME, tumor microenvironment; UMI, unique molecular identifiers; VEGF, vascular endothelial growth factor.
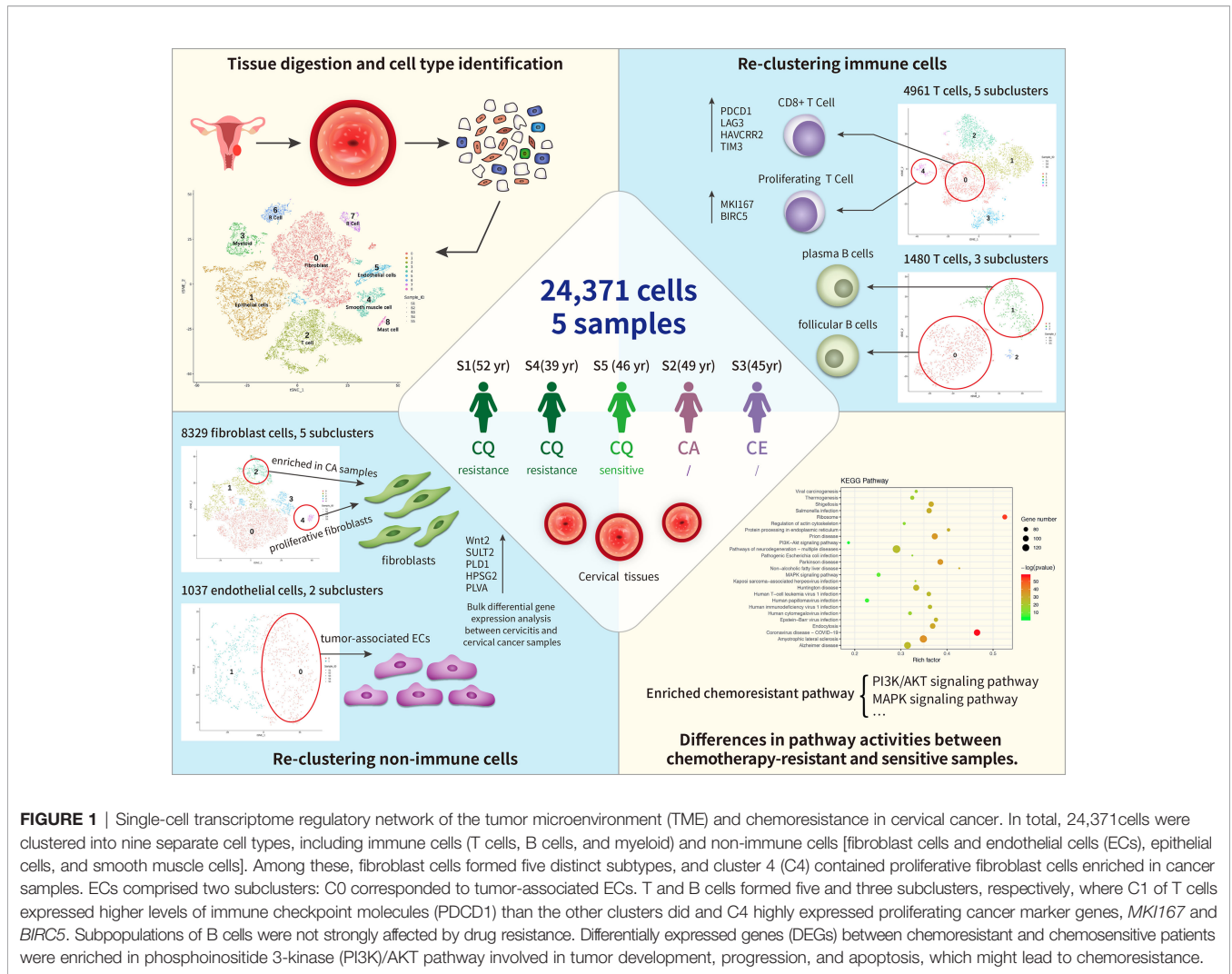
FIGURE 1 | Single-cell transcriptome regulatory network of the tumor microenvironment (TME) and chemoresistance in cervical cancer. In total, 24,371 cells were clustered into nine separate cell types, including immune cells (T cells, B cells, and myeloid) and non-immune cells [fibroblast cells and endothelial cells (ECs), epithelial cells, and smooth muscle cells]. Among these, fibroblast cells formed five distinct subtypes, and cluster 4 (C4) contained proliferative fibroblast cells enriched in cancer samples. ECs comprised two subclusters: C0 corresponded to tumor-associated ECs. T and B cells formed five and three subclusters, respectively, where C1 of T cells expressed higher levels of immune checkpoint molecules (PDCD1) than the other clusters did and C4 highly expressed proliferating cancer marker genes, *MKI167* and *BIRC5*. Subpopulations of B cells were not strongly affected by drug resistance. Differentially expressed genes (DEGs) between chemoresistant and chemosensitive patients were enriched in phosphoinositide 3-kinase (PI3K)/AKT pathway involved in tumor development, progression, and apoptosis, which might lead to chemoresistance.

Human Cervical Cancer Tissue Cell Dissociation

All fresh cervical cancer tissues were transferred from the operating room to the dissociation laboratory in cold Hank's balanced salt solution (HBSS) medium supplemented with 1% penicillin–streptomycin within 30 min. Samples were gently washed in phosphate-buffered saline (PBS) after removing the adipose tissue and minced into pieces of approximately 1 mm^3 using an Iris scissors. Enzymatic digestion was performed using the MACS tumor dissociation kit (Miltenyi Biotec) according to

TABLE 1 | Clinical information of the five patients.

	Patient 1	Patient 2	Patient 3	Patient 4	Patient 5
Sex	Female	Female	Female	Female	Female
Age	52	49	45	39	46
Chemotherapy before sampling	No	No	No	No	No
Chemotherapy drug	PTX + CBP	No	No	PTX + CBP	PTX + CBP
Clinical AJCC	Squamous-cell carcinoma (IIA2)	Adenocarcinoma	Cervicitis	Squamous-cell carcinoma (IIA2)	Squamous-cell carcinoma (IIA2)
Drug tolerance	Primary resistance	Non-chemotherapy	Non-chemotherapy	Primary resistance	Non-resistance
Other information	/	/	/	/	/
HPV infection	31 (+)	18 (+)	Negative	Negative	18 (+)

PTX, paclitaxel; CBP, carboplatin; HPV, human papillomavirus.

the instructions of the manufacturer. The cell suspension was further filtered through a 40-μm cell-strainer (BD) and centrifuged at 400g for 10 min to remove the cell aggregates. After removing the supernatant, the pelleted cells were resuspended in 2 ml red blood cell lysis buffer (SolarBio), and then resuspended in PBS with 10% fetal bovine serum (FBS). The viability of the obtained single-cell suspension was detected using a hemocytometer with trypan blue (0.4%, 420301, Gibco).

Single-Cell RNA Capturing, Library Preparation, and Sequencing

All single-cell capturing and downstream library construction were performed using the 10× Chromium Single Cell platform (Single Cell 3 library and Gel Bead kit v.3). Briefly, the cell suspensions at a concentration of 1,000 cells/μl were loaded into a 10x Genomics microfluidics chip and encapsulated with barcoded gel beads to generate gel beads in emulsion (GEM).

Reverse transcription of generated droplets was performed at 53°C for 45 min. cDNA was amplified for 12 cycles total on T100 Thermal Cycler (Bio-Rad). Then, RT-cDNA was recovered using Recovery Agent provided by 10× Genomics and purified with DynaBeads MyOne Silane Beads (Thermo Fisher Scientific) as outlined in the user guide. Subsequently, purified cDNAs were amplified and cleaned up with the SPRIselect Reagent Kit (Beckman Coulter, USA). Quantification of constructed libraries of each sample was detected using a Qubit2.0 Fluorometer (Invitrogen) before pooling. Pooled libraries were sequenced to a depth of an average of 50,000 reads per cell on a NovaSeq 6000 sequencer (Illumina, San Diego) at 2×150 bp sequencing model (23–25).

scRNA-Seq Data Analysis

scRNA-seq raw data were demultiplexed to FASTQ files (observed average read depth per cell was ~1.6 million reads) and aligned to an indexed ensembl_92-GRCh38.92 RefSeq genome to generate gene expression matrices using 10× Genomics pipeline CellRanger v.2.1.0 (25). The number of unique molecular identifiers (UMIs), the number of genes, and the percentage of mitochondrial genes were examined for quality control. Cells expressing <500 or >4,000 genes (potential cell duplets) and gene expression not detected in fewer than three cells were trimmed from the library.

Cells containing >10% mitochondrial genes were also discarded because of their poor cell viability (**Table S1**). We detected 92,675 genes in 21,433 cells from five samples. After data normalization, variably expressed genes were normalized and scaled, where single-cell gene counts were normalized to the total gene counts presented in that cell at a normalized expression between a low cutoff of 0.0125 and a high cutoff of 3 and a quantile-normalized variance >0.5, using the Seurat R package. The resulting gene expression values were transformed into a log space.

Major Cell-Type Clustering

Principal component analysis (PCA) was used to reduce the dimensionality of the results of variably expressed genes based on the JackStraw function. Then, the first 10 principal components

were selected as a statistically significant input for further two-dimensional visualization using t-distributed stochastic neighbor embedding (t-SNE) plots (RunTSNE function, the default setting). Cell clusters were annotated and identified to known cell types using specific marker genes identified using the Seurat "FindAllMarkers" function with the default setting (26).

Marker Gene and Cell-Type Identification

Cluster-specific genes were acquired using the Seurat native FindMarkers function with a log-fold change threshold of 0.25. Receiver operating characteristic (ROC) analysis was used to identify cell markers. To further characterize these cell types in each cluster, we used the automated annotation tool SingleR (27) and manually checked using known cell surface markers based on related references.
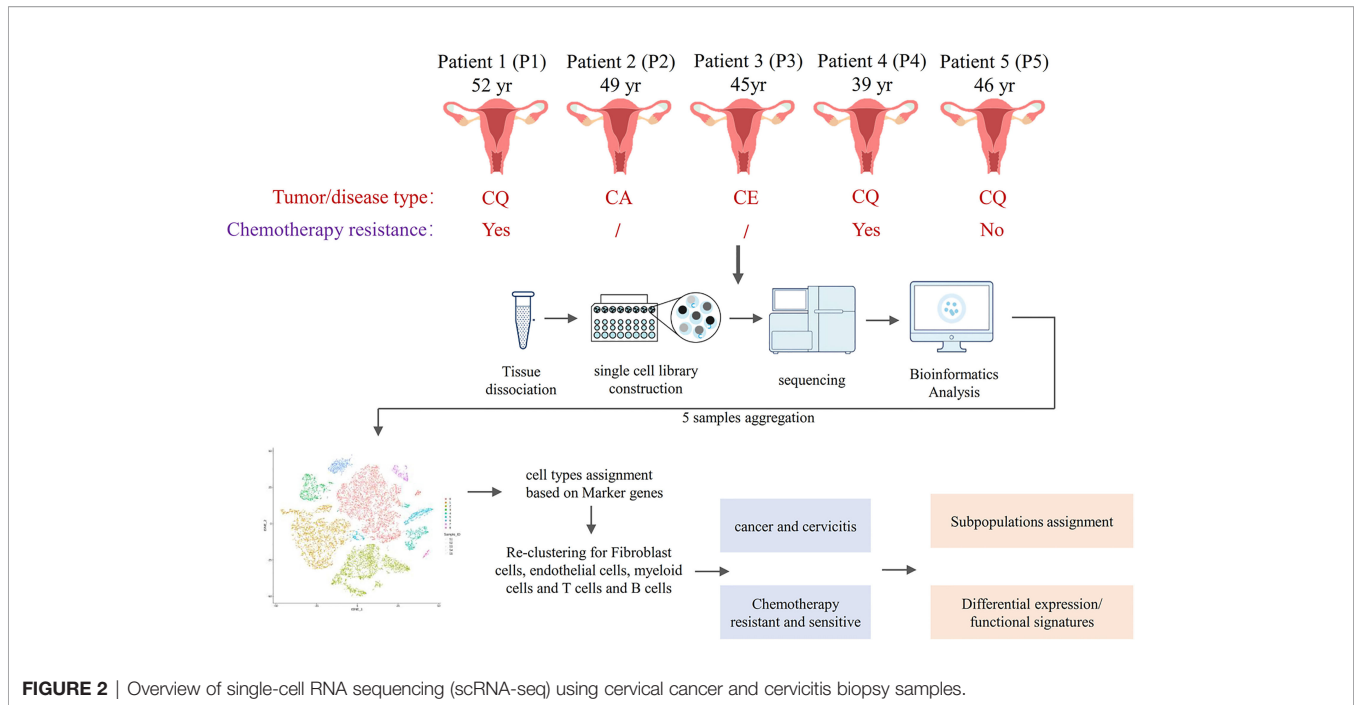
Identification of Differential Gene Expression and Cell Function in Different Samples

Differential expression analysis was performed after normalization and removal of the batch effects of total genes from the specific cluster from different samples. The function of *FindAllMarkers* wrapped in the R package of Seurat was used to identify differentially expressed genes for each of cell clusters compared to others. Then, the functions of *FindIntegrationAnchors* and *IntegrateData* wrapped in the R package of Seurat were employed to remove the batch effect referred to the standard procedure. We detected differentially expressed genes (DEGs) with a false discovery rate (FDR) <10e-6 and abs (log2 ratio) >2. Gene Ontology (GO) and Kyoto Encyclopedia of Genes and Genomes (KEGG) pathway analyses were performed to investigate the cell functional status. DEGs and molecular regulators in the clusters were investigated using GO and KEGG pathway analyses, respectively. GO and KEGG terms with an FDR <0.05 were considered significantly enriched (28).

RESULTS

Single-Cell Profiling of Cervical Cancer and Chronic Cervicitis Tissues

The single-cell atlas of the cervical tissues was characterized using five biopsy samples comprising three cervical squamous cell carcinomas (CQ), one cervical adenocarcinoma (CA), and one chronic cervicitis (CE). Two of the CQ patients were chemoresistant, one was chemosensitive, and three were infected with human papillomavirus. Each sample was processed to isolate single cells without prior selection of cell types, and then we performed scRNA-seq using a 10× Genomics Chromium platform to generate RNA-seq data. After quality filtering, 24,371 high-quality cells from five cervical biopsy samples with a median of 1,303–2,214 genes per cell were analyzed (**Figure 2**). Subsequently, the cells were further identified to be nine separate cell types, including fibroblast cells (34.17%), epithelial cells (24.07%), smooth muscle cells (4.3%), ECs (4.26%), and immune cells (33.2%).

FIGURE 2 | Overview of single-cell RNA sequencing (scRNA-seq) using cervical cancer and cervicitis biopsy samples.

The main cell types were identified based on gene expression patterns obtained using dimensionality reduction and unsupervised cell clustering with the described Seurat pipeline. Based on the marker genes of each cell cluster, nine distinct cell clusters were assigned to known cell lineages, which mainly comprised immune and non-immune cells (**Figure 3A**). The t-SNE plot also showed distinct clustering according to the tumor origin (**Figure 3B**). The heatmap showed differentially expressed marker genes in nine clusters (**Figure 3C**).

The proportions and composition of cell types varied among the different samples. The CA samples clustered with CE samples and mainly comprised fibroblast cells, accounting for 84.7% and 63.4% of the total cells. In contrast, the corresponding CQ werepredominantly epithelial and immune cells with almost no fibroblasts and ECs. Immune cells mainly consisted of B cells [CD20 (MS4A1) and CD79A] (26, 29, 30), myeloid cells (IL1B) (29), T cells (CD3D, CD2) (29–31), and mast cells (MS4A2) (29). The non-immunecell lineages comprised fibroblasts (DCN, LUM, and COL1A2) (26, 32, 33), epithelial cells (KRT, SLPI, and SFN) (32, 34), smooth muscle cells (MYL9, CALD1, and RGS5) (35, 36), andECs [VMF, ENG, and fms-related receptor tyrosine kinase 1 (FLT1)] (26) (**Figures 3D–F**).

Reclustering and Differential Gene Profiles of Fibroblast and ECs in Cervicitis and Cervical Cancer Samples

We detected 8,329 fibroblast cells among the five samples and most were found in the CA and the CE samples, which accounted for 95.1% of the total fibroblast cells of the five samples (**Figure 4A**). To gain a better understanding of these cell types, we performed a reclustering of 8,329 fibroblasts and

1,037 ECs and assigned each of these subclusters based on known cell markers.

In our study, five distinct subtypes of fibroblast cells were identified. Cluster 0 (C0), C1, and C3 contained cells from all samples, but C2 and C4 were strongly enriched in the CA sample (**Figure 4B**). C0 and C3 were similar, corresponding to cells expressing extracellular matrix (ECM) molecules, such as collagen type III alpha 1 chain (COL3A1), COL6A3, and COL1A1, and these cells represent a population of collagen-generating fibroblasts. C1 demonstrated differential activation of FOS, heat shock protein 90 (HSP90s), and ETS-related gene-1 (ERG1).

Cells in C2 exhibited differentially elevated expression of genes involved in translation initiation [ribosomal protein L10 (RPL10) and RPS3] (37) and iron metabolism regulation [ferritin light chains (FTLs)] (38). The final subpopulation C4 was speculated to be a group of proliferative fibroblast cells, which has not been previously recognized, based on the expression of a relatively high level of proliferative genes such as the *S100* (*s100B*) and *CDH19* genes (18, 39) (**Figure 4C**).

To better understand the differential gene expression profiles between cervicitis and cervical cancer samples, bulk differential gene expression analysis was performed for cervical cancer and cervicitis samples. The two-tailed Wilcoxon rank-sum test, which is implemented in R, was used to conduct the bulk differential gene expression analysis. The volcano map (**Figure 4D**) and the heat map (**Figure 4E**) showed significant diversity in the expressed genes across the two samples.. For example, wnt2, a member of the WNT gene family, is highly expressed in cervical cancer samples, and WNT signaling is normally involved in the development and progression of various cancers.
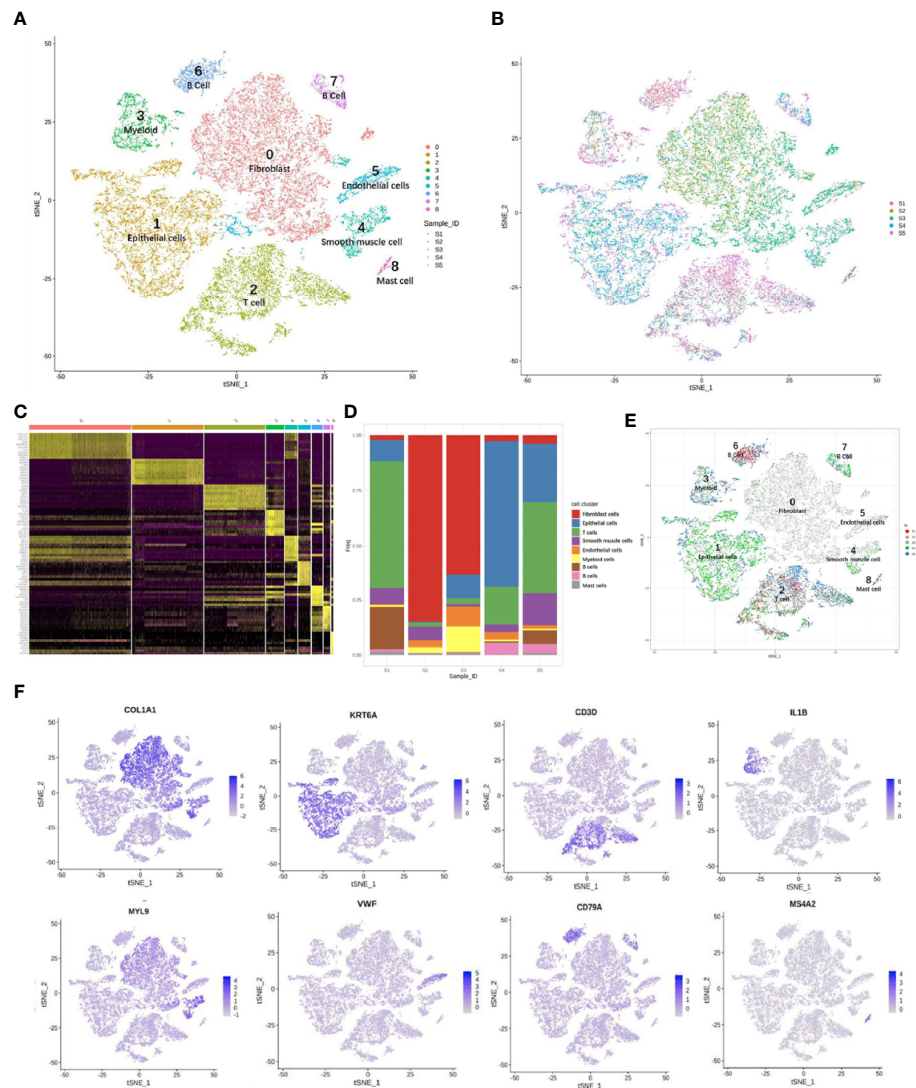
FIGURE 3 | Overview of 24,371 cells from five cervical cancer tissues. *t*-Distributed stochastic neighbor embedding (*t*-SNE) plots displaying 24,371 cell profiles with each cell color-coded for **(A)** associated cell type and **(B)** its sample origin. **(C)** Heatmap shows differentially expressed marker genes (rows) in nine clusters. Yellow and dark purple: high and low expression, respectively. **(D)** Proportions of cells in each sample. **(E)** *t*-SNE plots displaying 24,371 cell profiles with color-coded sample origins. Samples 2 and 3 are gray. **(F)** *t*-SNE plot color-coded for marker gene expression (gray to white to blue) for *COL1A2* (cluster 0, C0), *KRT6A* (C1), *CD3D* (C2), *IL1B* (C3), *MYL9* (C4), *VWF* (C5), *CD79A* (C6 and C7), and *MS4A2* (C8).

We also found that the extracellular sulfatase, SULT2, was highly expressed in the cancer samples, which is consistent with the findings of other studies (40). Upregulation of *SULF2* gene expression is associated with proliferation, invasion, and migration of cervical cancer cells by its regulation of the extracellular signal-related kinase (ERK)/AKT signaling pathway (41). The ECM is important in tumor genesis and progression and fibroblast-activating protein (FAP), which plays a crucial role in ECM production and remodeling genes and is highly upregulated in tumor fibroblast cells (42).

C4 mainly contained proliferative fibroblast cells, which were mostly from the CA sample. Furthermore, we studied the gene profiles and performed functional enrichment, which

demonstrated that several crucial genes were upregulated or downregulated in this cluster. The functional enrichment analysis results indicated that C4 was enriched in cell adhesion molecule binding and collagen-binding growth factor binding in molecular functions (**Figure 4F**).

As shown in **Figures 5A–C**, the 1,037 ECs were clustered in two separate subclusters. C0 corresponded to tumor-associated [heparan sulfate proteoglycan 2 (HPSG2) and plasmalemmal vesicle-associated protein (PLVAP)] and C1 ECs were blood ECs (FLT). Cells from sample 2 were spread in C0 but not in C1. PLVAP is located in the fenestral diaphragm and is considered to play a role in the passage of proteins through the fenestrae (43, 44). The generation of *Plvap*-deficient mice has highlighted the
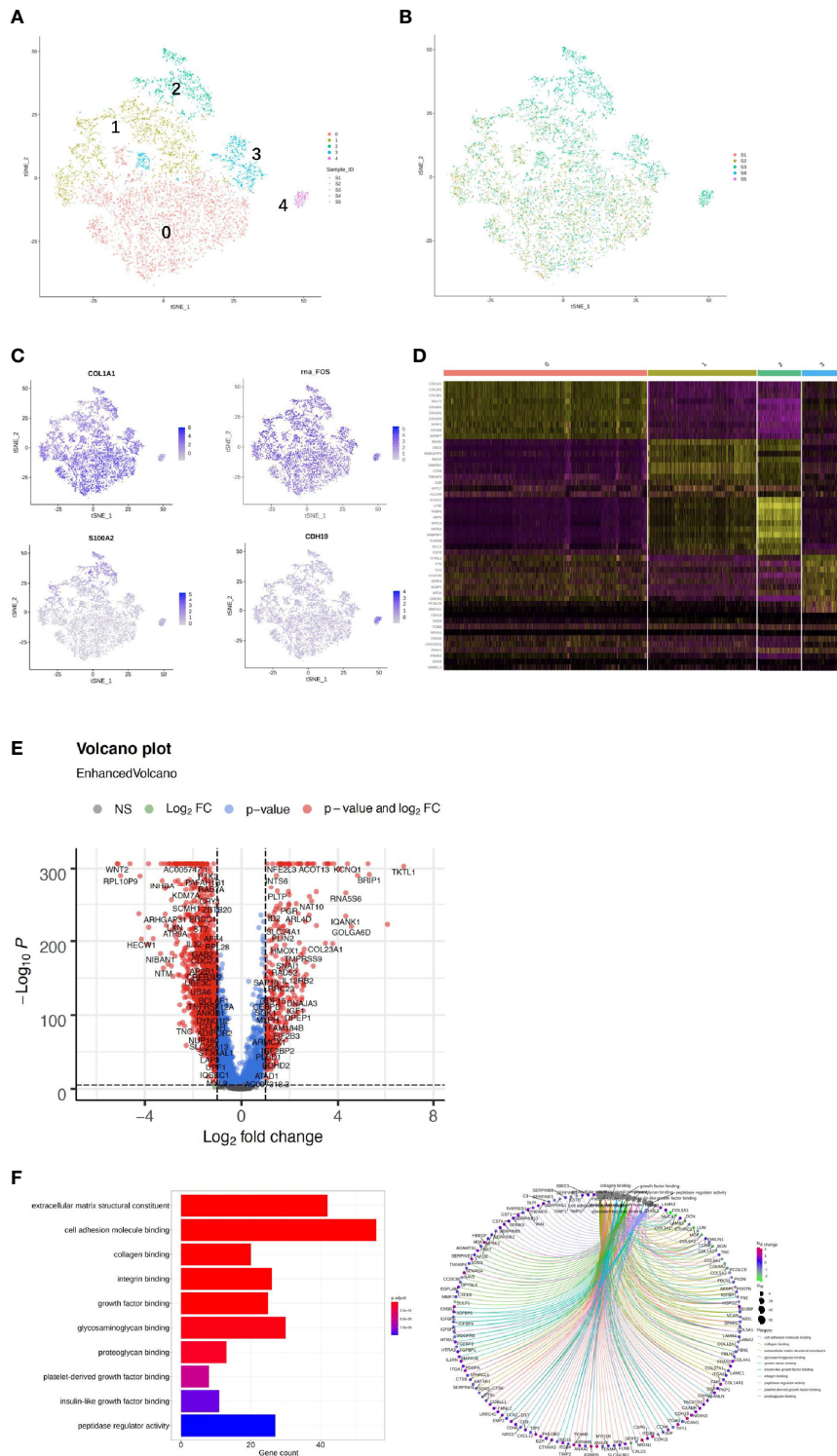
FIGURE 4 | Single-cell RNA sequencing (scRNA) profiles of fibroblast cell lineages. Reclustering of 8,329 fibroblast cells color-coded by (A) clusters and (B) sample origin (right). (C) *t*-Distributed stochastic neighbor embedding (*t*-SNE) plot color-coded for marker gene expression (gray to white to blue) for *COLIAI*, *FOS*, *S100A2*, and *CDH19*. (D) Heatmap shows differentially expressed marker genes (rows) in five clusters. Yellow and dark purple: high and low expression, respectively. (E) Volcano plot shows differentially expressed marker genes between cervicitis and cervical cancer samples. (F) Differences in pathway activities of cells between cluster 1 (C1), C2, C3, and C4.
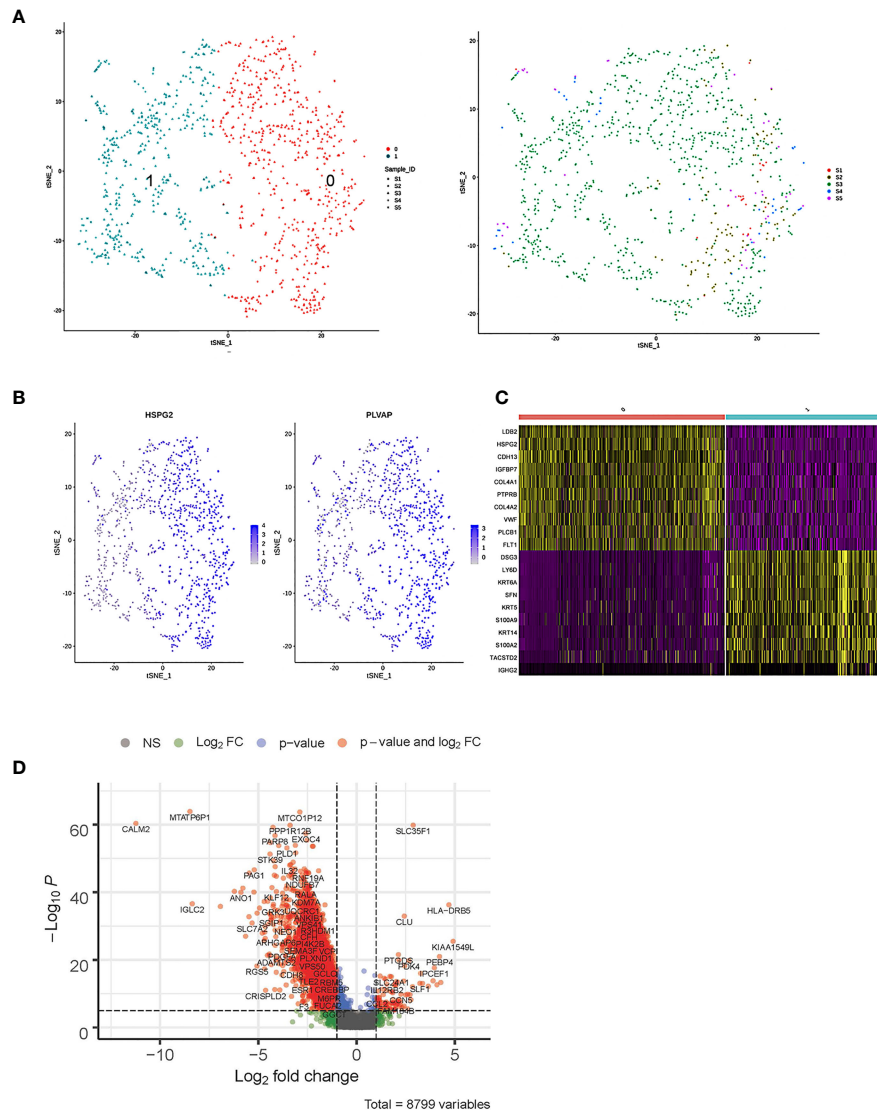
FIGURE 5 | Single-cell RNA sequencing (scRNA) profiles of endothelial cell (EC) lineages. **(A)** Reclustering of 1,037 fibroblast cells, color-coded by clusters (left) or sample origin (right). **(B)** *t*-Distributed stochastic neighbor embedding (*t*-SNE) plot color-coded for marker gene expression (gray to white to blue) of *HPSG2* and *PLVAP*. **(C)** Heatmap shows differentially expressed marker genes (rows) in two clusters. Yellow and dark purple: high and low expression, respectively. **(D)** Volcano plot shows differentially expressed marker genes between cervicitis and cervical cancer samples.

structural role of PLVAP in the maintenance of size-selective permeability in fenestrated endothelia (45, 46). Moreover, *Plvap*-deficient mice that survived postnatally showed growth retardation (46).

The bulk differential gene expression analysis between cervicitis and cervical cancer samples showed that several cancer marker genes, which have been reported in various malignant tumors responsible for angiogenesis, metastasis, and invasion, were significantly elevated in cancer ECs (**Figure 5D**). For example, we detected elevated levels of phospholipase D1 (PLD1), a key enzyme involved in lipid metabolism, indicating that abnormal lipid metabolism might be involved in the tumorigenesis and progression of cervical cancer (47, 48).

Acquired Resistance Was Associated With Differential Immune Cell Subpopulation Distribution and mRNA Expression

Both adaptive immune cells (T and B lymphocytes) and innate immune cells (such as macrophages, mast cells, neutrophils, dendritic cells, and natural killer cells) have critical roles in the TME and are considered to interact with tumor cells by direct contact or through different chemokine and cytokine signaling pathways that regulate the response of tumors to therapy. To explore the diversity of immune cells in cervical cancer, we extracted 4,961 T cells, 1,480 B cells, and 1,476 myeloid cells from three individual CQ patients and reclustered them (**Figures 6**, **7**). Furthermore, the main T-cell clusters could be
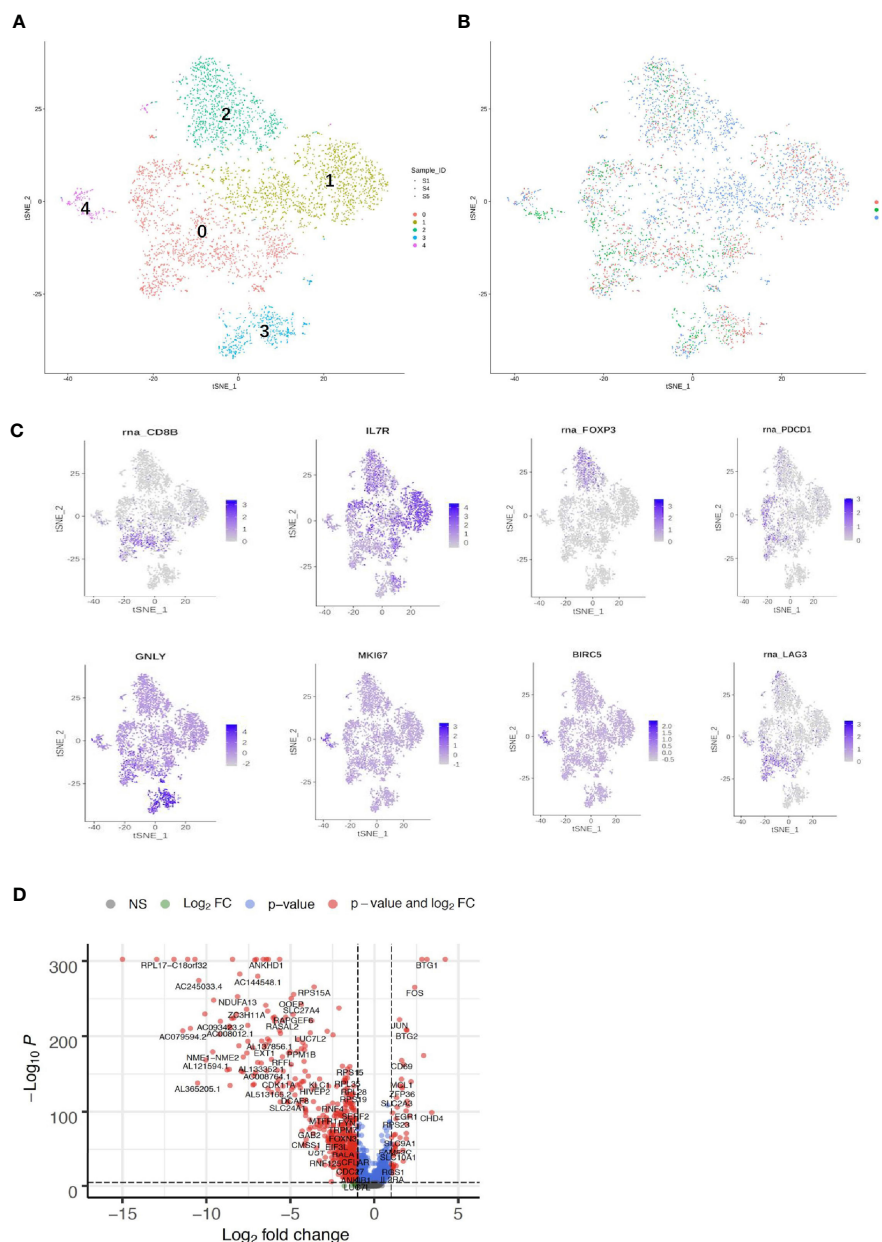
FIGURE 6 | Single-cell RNA sequencing (scRNA) profiles of T-cell lineages. Reclustering of 4,961 T cells color-coded by **(A)** clusters and **(B)** sample origin (right). **(C)** *t*-Distributed stochastic neighbor embedding (*t*-SNE) plot color-coded for marker gene expression (gray to white to blue) for *CD8+* (cluster 0, C0), *CD4+* (C1), *IL2A* (C2), *GNLY* (C3), *MKI67*, and *BIRC2* (C4). **(D)** Volcano plot shows differentially expressed marker genes (rows) between chemoresistant patients and chemosensitive samples.

classified into five subpopulations designated as T0–T4, which were cytotoxic CD8+ T cells (CD8A+ and CD8B), CD4+ T cells [CD4+ and interleukin 7R (IL7R)], regulatory T cells [IL2RA, forkhead box protein P3 (FOXP3), tumor necrosis factor receptor superfamily, member 4 (TNFRSF4)], natural killer cells [killer cell lectin-like receptor C1 (KLRC1), X-C motif chemokine ligand 1/2 (XCL1/2), and granulysin (GNLY)], and proliferating T cells [marker of proliferation Ki-67 (MKI67) and

baculoviral IAP repeat containing 5 (BIRC5), **Figure 5A**] (26, 29). Cells from all clusters were detected in all patients. Cells from all five clusters were detected in both chemoresistant and chemosensitive patients, except for C1, which was predominantly derived from chemoresistant patients. It is worth noting that there were high levels of immune checkpoint molecules, including approved target programmed cell death 1 (PDCD1) and other targets that are currently undergoing clinical
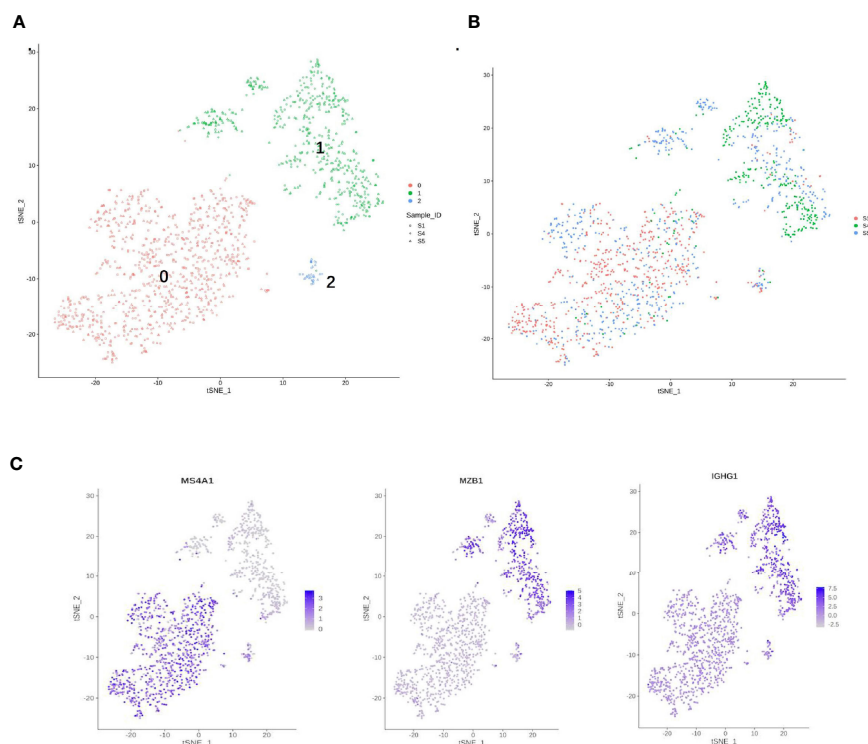
FIGURE 7 | Single-cell RNA sequencing (scRNA) profiles for B-cell lineages. **(A)** Reclustering of 1,480 B cells, color-coded by their cluster. **(B)** Its sample origin. **(C)** t-SNE plot color-coded for marker gene expression (gray to white to blue) for MS4A1 (cluster 0), MZB1, and IGHG1 (cluster 1).

trials [lymphocyte activating 3 (LAG3) and hepatitis A virus cellular receptor 2/T-cell immunoglobulin and mucin domain-3 (HAVCR2/TIM3)] (49), indicating that the cytotoxic activities of CD8+ are significantly curtailed by high-level expression of the checkpoint gene. The robust CD8+ response was confirmed to play a critical role in a mammary tumor model treated with a HER2 inhibitor (50). Additionally, the average expression of the proliferating cancer marker genes, *MKI167* and *BIRC5*, was significantly enriched in C4 (**Figure 6D**). These two cancer marker genes, *MKI167* and *BIRC5*, have been reported to be highly expressed in cervical cancer in many studies, where they are associated with the cell cycle pathway and cell apoptosis inhibition, respectively, and are both involved in breast cancer pathogenesis (51–53).

B cells (1,480) were detected and reclustering from C6 and C7 revealed three subclusters, and cell type assignments were performed based on known marker genes. C0 corresponded to follicular B cells based on marker MS4A1, whereas C1 corresponded to plasma B cells based on MZB1, CD38, and IGHG1 (**Figures 7A, C**) (29, 54). C2 contained lower quality B cells and showed no B-cell markers; thus, it was not further analyzed. One sample was mostly from patient 4, and two others were mostly from patients 1 and 5. The *t*-SNE profile failed to show the separation of subclusters between chemoresistant and chemosensitive patients, indicating that the B-cell subpopulation was not strongly affected by drug resistance.

DEG Pathways Between Chemoresistant and Chemosensitive Patients

To investigate the enriched functions of DEGs between chemoresistant and chemosensitive samples, signaling pathway analysis was performed among subpopulations of epithelial, T, and B cells. In total, 3,157, 1,399, and 1,141 DEGs were annotated into 327, 312, and 312 pathways for epithelial, T, and B cells, respectively, in the KEGG database (**Tables S2–S4**). The top 25 annotation results, which were classified according to the pathway types, are shown in **Figure 8**. Several signaling pathways that are closely correlated with chemotherapy were enriched in all three subpopulations, including the PI3K/AKT and mitogen-activated protein kinase (MAPK) signaling pathways. The PI3K/AKT signaling pathway is involved in tumor development, progression, cellular survival, and apoptosis, and its correlation with chemoresistance has been presented in numerous studies (55–57) and cervical cancer (12). Another chemotherapy resistance-associated pathway, the MAPK signaling pathway, was significantly enriched and upregulated in chemoresistant patients and is responsible for the regulation of cell migration, survival, proliferation, and progression (58). Activation of survival pathways involving PI3K/Akt and MAPK caused by integrins and soluble factors secreted in the TME results in elevated expression of anti-apoptotic proteins, leading to cell viability and drug resistance (7).
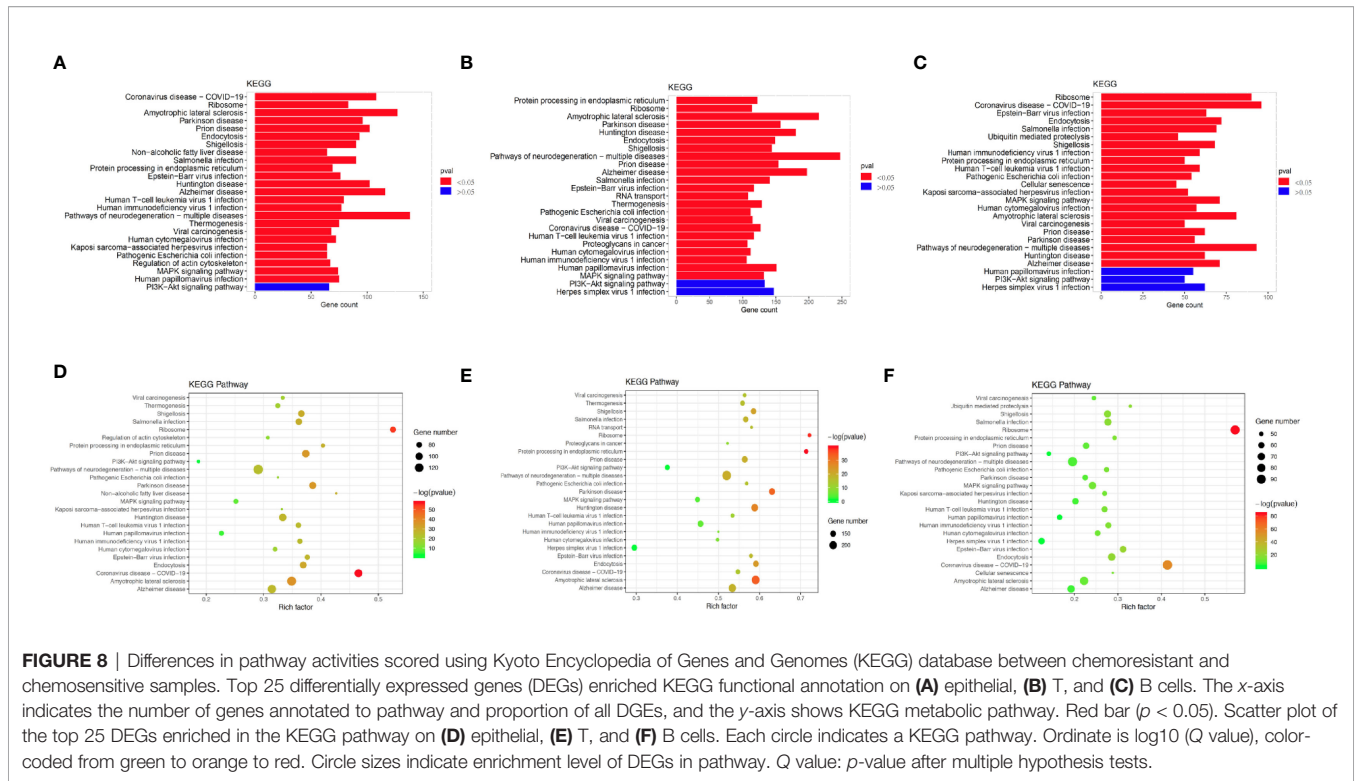
FIGURE 8 | Differences in pathway activities scored using Kyoto Encyclopedia of Genes and Genomes (KEGG) database between chemoresistant and chemosensitive samples. Top 25 differentially expressed genes (DEGs) enriched KEGG functional annotation on **(A)** epithelial, **(B)** T, and **(C)** B cells. The x-axis indicates the number of genes annotated to pathway and proportion of all DGEs, and the y-axis shows KEGG metabolic pathway. Red bar ($p < 0.05$). Scatter plot of the top 25 DEGs enriched in the KEGG pathway on **(D)** epithelial, **(E)** T, and **(F)** B cells. Each circle indicates a KEGG pathway. Ordinate is log10 (Q value), color-coded from green to orange to red. Circle sizes indicate enrichment level of DEGs in pathway. Q value: p-value after multiple hypothesis tests.

DISCUSSION

Advanced scRNA-seq technology has allowed the comprehensive investigation of tumor heterogeneity gene expression differences with single-cell resolution. Although scRNA-seq profiles of other gynecological cancers, including breast and ovarian cancers, have been extensively studied (18, 34, 59), profiles of the microenvironment of cervical cancer, particularly with respect to chemotherapy resistance, have not been demonstrated. To the best of our knowledge, this is one of the first few studies to comprehensively characterize a single-cell atlas of cervical cancer patients in China and worldwide (60).

Here, we present a comprehensive catalog of cell types and subtypes, including fibroblast, endothelial, and immune cells in CQ, adenocarcinoma, and non-tumorous CE biopsy samples at single-cell resolution. In this study, we isolated 24,371 cells from five cervical biopsy samples and identified nine separate cell types, including fibroblast, epithelial, smooth muscle, and immune cells as well as ECs. Then, we subclustered the main cell types into different subpopulations based on the expression of the marker gene. We then studied pathway signatures and activities of distinct subpopulations that represent different biological and molecular entities between cervical cancer and cervicitis samples, and assessed the differential gene expression and signaling pathways between chemoresistant and chemosensitive cervical cancer patients.

Fibroblasts are considered a heterogeneous population in many cancers, but the extent of heterogeneity remains unclear, especially in cervical cancer because they are difficult to culture and highly dependent on context (26). Furthermore, fibroblasts

are a large source of growth factors and cytokines, including stromal cell-derived factor 1 (SDF1), hepatocyte growth factor (HGF), and vascular endothelial growth factor (VEGF), which all promote tumor growth and contribute to chemotherapy resistance (61–63). Although most clusters were composed of cells originating from different samples, the fibroblast cells and ECs were observably enriched in CA and CE patients.

The significant shift might have occurred because the condition of the patients who provided the cervical squamous cell carcinoma samples was likely more serious, which would result in the recruitment of more immune cells to exert their antitumor function. In addition, upregulated expression of WNT2 in tumor fibroblast cells, which was observed in this study, could also result in tumor growth and promotion of invasion by activating the canonical WNT/β-catenin signaling pathway (64, 65). A previous study also revealed that downregulating WNT2 significantly suppressed cell motility and invasion and reversed epithelial–mesenchymal transition (EMT) progression in cervical cancer (66).

By comparing the differential gene expression in fibroblasts and ECs between cervical cancer and cervicitis patients, we found that several cancer marker genes, which have been reported in various malignant tumors responsible for angiogenesis, metastasis, and invasion, via various metabolic pathways related to cervical cancer, were significantly elevated in cancer ECs. For instance, genes involved in translation initiation such as RPL10 and RPS3 (37) and iron metabolism regulation such as FTLs (38), which have been reported to be involved in increased cell viability, migration, and invasion in different cancers, were elevated in the identified C2. This observation indicates that

these cells are highly active and associated with tumorigenesis. In addition, the differential activation of FOS, HSP90s, and ERG1 exhibited by the cells in C1 indicated a strong correlation with myogenesis and fibrosis (37, 67).

Tumor cells have been reported to trigger the immunosuppressive activities of tumor-associated ECs that influence therapeutic responses (68). ECs selectively permit transmigration of immunosuppressive myeloid cells from the blood to the tumor, thereby impairing antitumor immune responses (69). Moreover, ECs involved in the TME may also suppress T-cell function through the expression of different inhibitory molecules, such as programmed cell death ligand 1 (PDL1) and PDL2 (70).

Checkpoint immunotherapy is rarely used in cervical cancer, and there is a poor understanding of the outcome of immunotherapy. The results of this study were consistent with this phenomenon, and we found that the immune checkpoint molecules, PDCD1, LAG3, and HAVCR2, were highly expressed in CD8+ cells. This observation indicates that cytotoxicity was inhibited by high checkpoint expression (54) and that immunotherapy could also be useful in cervical cancer by targeting these pathways. This result is in agreement with the good clinical results observed in immunotherapy of cervical cancer (71).

The results of the analysis of differentially enriched signaling pathways did not show significant differences in chemoresistant patients. However, the PI3K/AKT pathway enriched most DEGs, which suggests that the activation state of this common pathway, which is involved in tumor development, progression, and apoptosis, might contribute to the development of resistance to chemotherapy in cervical cancer patients. Inhibition of certain components of the PI3K/AKT and MAPK pathways not only enhances chemotherapy efficacy in cervical cancer, but also has the potential to overcome resistance (72, 73).

There are some limitations to our study that need to be addressed in future studies. First, because sample collection was challenging, the number of samples in this study was relatively small, especially the chemoresistant and chemosensitive samples, which indicates that our observations cannot reflect the comprehensive profiles of the TME and generalize the gene expression differences in cervical cancer and its chemoresistant features.

CONCLUSION

In conclusion, we comprehensively described the profiles of immune and non-immune cells in cervical cancer and cervicitis samples at single-cell resolution. Furthermore, we compared the distinctive features of signaling pathways among subpopulations from chemoresistant and chemosensitive samples in this study. Our results of the analysis of extensive bioinformatics data demonstrated the scope and potential impact of heterogeneity and suggest that single-cell profiling could identify and characterize clinically important subpopulations to develop successful targeted treatments. Our findings also indicated the need for comprehensive single-cell gene profiling

and characterization of heterogeneous tumors such as chemoresistant cervical cancer. Finally, by assessing the cell subpopulations, differential gene expression between chemoresistant and chemosensitive samples, and distinct signaling pathways, we expect that our findings will provide novel and deeper insights into human cervical cancer and facilitate the advancement of its diagnosis and treatment.

DATA AVAILABILITY STATEMENT

The original contributions presented in the study are included in the article/**Supplementary Material**. Further inquiries can be directed to the corresponding authors.

ETHICS STATEMENT

The studies involving human participants were reviewed and approved by the Institutional Review Board of Renmin Hospital of Wuhan University (Institutional Review Board no. WDRY2021-K014). The patients/participants provided their written informed consent to participate in this study.

AUTHOR CONTRIBUTIONS

Conceived and designed the experiments: CS, XL, and MG. Acquired the data: MG, TH, YY, and SD. Analyzed and interpreted the data: MG, TH, and YY. Drafted the manuscript: MG and TH. Obtained funding: CS. Supervised the study: CS and XL. All authors contributed to the article and approved the submitted version.

FUNDING

ACKNOWLEDGMENTS

SUPPLEMENTARY MATERIAL

The Supplementary Material for this article can be found online at: https://www.frontiersin.org/articles/10.3389/fonc.2021.753386/full#supplementary-material

REFERENCES

1. Arbyn M, Weiderpass E, Bruni L, de Sanjose S, Saraiya M, Ferlay J, et al. Estimates of Incidence and Mortality of Cervical Cancer in 2018: A Worldwide Analysis. *Lancet Glob Health* (2020) 8(2):e191–203. doi: 10.1016/S2214-109X(19)30482-6

2. Rosen VM, Guerra I, McCormack M, Nogueira-Rodrigues A, Sasse A, Munk VC, et al. Systematic Review and Network Meta-Analysis of Bevacizumab Plus First-Line Topotecan-Paclitaxel or Cisplatin-Paclitaxel Versus Non-Bevacizumab-Containing Therapies in Persistent, Recurrent, or Metastatic Cervical Cancer. *Int J Gynecol Cancer* (2017) 27(6):1237–46. doi: 10.1097/IGC.0000000000001000

3. Kitagawa R, Katsumata N, Shibata T, Kamura T, Kasamatsu T, Nakanishi T, et al. Paclitaxel Plus Carboplatin Versus Paclitaxel Plus Cisplatin in Metastatic or Recurrent Cervical Cancer: The Open-Label Randomized Phase III Trial Jcog0505. *J Clin Oncol* (2015) 33(19):2129–35. doi: 10.1200/JCO.2014.58.4391

4. Markman M. Advances in Cervical Cancer Pharmacotherapies. *Expert Rev Clin Pharmacol* (2014) 7(2):219–23. doi: 10.1586/17512433.2014.884924

5. Quail DF, Joyce JA. Microenvironmental Regulation of Tumor Progression and Metastasis. *Nat Med* (2013) 19(11):1423–37. doi: 10.1038/nm.3394

6. Hanahan D, Coussens LM. Accessories to the Crime: Functions of Cells Recruited to the Tumor Microenvironment. *Cancer Cell* (2012) 21(3):309–22. doi: 10.1016/j.ccr.2012.02.022

7. Wu T, Dai Y. Tumor Microenvironment and Therapeutic Response. *Cancer Lett* (2017) 387:61–8. doi: 10.1016/j.canlet.2016.01.043

8. Gottesman MM, Ludwig J, Xia D, Szakacs G. Defeating Drug Resistance in Cancer. *Discovery Med* (2006) 6(31):18–23.

9. Cadron I, Van Gorp T, Amant F, Leunen K, Neven P, Vergote I. Chemotherapy for Recurrent Cervical Cancer. *Gynecol Oncol* (2007) 107 (1 Suppl 1):S113–8. doi: 10.1016/j.ygyno.2007.07.004

10. Siddik ZH. Cisplatin: Mode of Cytotoxic Action and Molecular Basis of Resistance. *Oncogene* (2003) 22(47):7265–79. doi: 10.1038/sj.onc.1206933

11. Rhodes DR, Chinnaiyan AM. Integrative Analysis of the Cancer Transcriptome. *Nat Genet* (2005) 37(Suppl):S31–7. doi: 10.1038/ng1570

12. Wang Y, Liu L, Chen Z. Transcriptome Profiling of Cervical Cancer Cells Acquired Resistance to Cisplatin by Deep Sequencing. *Artif Cells Nanomed Biotechnol* (2019) 47(1):2820–9. doi: 10.1080/21691401.2019.1637882

13. Fan Z, Cui H, Yu H, Ji Q, Kang L, Han B, et al. MiR-125a Promotes Paclitaxel Sensitivity in Cervical Cancer Through Altering STAT3 Expression. *Oncogenesis* (2016) 5:e223. doi: 10.1038/oncsis.2016.21

14. Guo X, Zhang Y, Zheng L, Zheng C, Song J, Zhang Q, et al. Global Characterization of T Cells in Non-Small-Cell Lung Cancer by Single-Cell Sequencing. *Nat Med* (2018) 24(7):978–85. doi: 10.1038/s41591-018-0045-3

15. Gladka MM, Molenaar B, de Ruiter H, van der Elst S, Tsui H, Versteeg D, et al. Single-Cell Sequencing of the Healthy and Diseased Heart Reveals Cytoskeleton-Associated Protein 4 as a New Modulator of Fibroblasts Activation. *Circulation* (2018) 138(2):166–80. doi: 10.1161/CIRCULATIONAHA.117.030742

16. Ofengeim D, Giagtzoglou N, Huh D, Zou C, Yuan J. Single-Cell RNA Sequencing: Unraveling the Brain One Cell at a Time. *Trends Mol Med* (2017) 23(6):563–76. doi: 10.1016/j.molmed.2017.04.006

17. Fattore L, Ruggiero CF, Liguoro D, Mancini R, Ciliberto G. Single Cell Analysis to Dissect Molecular Heterogeneity and Disease Evolution in Metastatic Melanoma. *Cell Death Dis* (2019) 10(11):827. doi: 10.1038/s41419-019-2048-5

18. Shih AJ, Menzin A, Whyte J, Lovecchio J, Liew A, Khalili H, et al. Identification of Grade and Origin Specific Cell Populations in Serous Epithelial Ovarian Cancer by Single Cell RNA-Seq. *PLoS One* (2018) 13(11): e0206785. doi: 10.1371/journal.pone.0208778

19. Bian S, Hou Y, Zhou X, Li X, Yong J, Wang Y, et al. Single-Cell Multiomics Sequencing and Analyses of Human Colorectal Cancer. *Science* (2018) 362 (6418):1060–3. doi: 10.1126/science.aao3791

20. Xu J, Liao K, Yang X, Wu C, Wu W, Han S. Using Single-Cell Sequencing Technology to Detect Circulating Tumor Cells in Solid Tumors. *Mol Cancer* (2021) 20(1):104. doi: 10.1186/s12943-021-01392-w

21. Xu Y, Su GH, Ma D, Xiao Y, Shao ZM, Jiang YZ. Technological Advances in Cancer Immunity: From Immunogenomics to Single-Cell Analysis and Artificial Intelligence. *Signal Transduct Target Ther* (2021) 6(1):312. doi: 10.1038/s41392-021-00729-7

22. Devitt K, Hanson SJ, Tuong ZK, McMeniman E, Soyer HP, Frazer IH, et al. Single-Cell RNA Sequencing Reveals Cell Type-Specific HPV Expression in Hyperplastic Skin Lesions. *Virology* (2019) 537:14–9. doi: 10.1016/j.virol.2019.08.007

23. Xie T, Wang Y, Deng N, Huang G, Taghavifar F, Geng Y, et al. Single-Cell Deconvolution of Fibroblast Heterogeneity in Mouse Pulmonary Fibrosis. *Cell Rep* (2018) 22(13):3625–40. doi: 10.1016/j.celrep.2018.03.010

24. Januszyk M, Chen K, Henn D, Foster DS, Borrelli MR, Bonham CA, et al. Characterization of Diabetic and Non-Diabetic Foot Ulcers Using Single-Cell RNA-Sequencing. *Micromachines (Basel)* (2020) 11(9):815–30. doi: 10.3390/mi11090815

25. Macosko EZ, Basu A, Satija R, Nemesh J, Shekhar K, Goldman M, et al. Highly Parallel Genome-Wide Expression Profiling of Individual Cells Using Nanoliter Droplets. *Cell* (2015) 161(5):1202–14. doi: 10.1016/j.cell.2015.05.002

26. Lambrechts D, Wauters E, Boeckx B, Aibar S, Nittner D, Burton O, et al. Phenotype Molding of Stromal Cells in the Lung Tumor Microenvironment. *Nat Med* (2018) 24(8):1277–89. doi: 10.1038/s41591-018-0096-5

27. Aran D, Looney AP, Liu L, Wu E, Fong V, Hsu A, et al. Reference-Based Analysis of Lung Single-Cell Sequencing Reveals a Transitional Profibrotic Macrophage. *Nat Immunol* (2019) 20(2):163–72. doi: 10.1038/s41590-018-0276-y

28. Chen EY, Tan CM, Kou Y, Duan Q, Wang Z, Meirelles GV, et al. Enrichr: Interactive and Collaborative HTML5 Gene List Enrichment Analysis Tool. *BMC Bioinf* (2013) 14:128. doi: 10.1186/1471-2105-14-128

29. Cai Y, Dai Y, Wang Y, Yang Q, Guo J, Wei C, et al. Single-Cell Transcriptomics of Blood Reveals a Natural Killer Cell Subset Depletion in Tuberculosis. *EBioMedicine* (2020) 53:102686. doi: 10.1016/j.ebiom.2020.102686

30. Zhao J, Guo C, Xiong F, Yu J, Ge J, Wang H, et al. Single Cell RNA-Seq Reveals the Landscape of Tumor and Infiltrating Immune Cells in Nasopharyngeal Carcinoma. *Cancer Lett* (2020) 477:131–43. doi: 10.1016/j.canlet.2020.02.010

31. Chen YP, Yin JH, Li WF, Li HJ, Chen DP, Zhang CJ, et al. Single-Cell Transcriptomics Reveals Regulators Underlying Immune Cell Diversity and Immune Subtypes Associated With Prognosis in Nasopharyngeal Carcinoma. *Cell Res* (2020) 30(11):1024–42. doi: 10.1038/s41422-020-0374-x

32. McCray T, Moline D, Baumann B, Vander Griend DJ, Nonn L. Single-Cell RNA-Seq Analysis Identifies a Putative Epithelial Stem Cell Population in Human Primary Prostate Cells in Monolayer and Organoid Culture Conditions. *Am J Clin Exp Urol* (2019) 7(3):123–38.

33. He H, Suryawanshi H, Morozov P, Gay-Mimbrera J, Del Duca E, Kim HJ, et al. Single-Cell Transcriptome Analysis of Human Skin Identifies Novel Fibroblast Subpopulation and Enrichment of Immune Subsets in Atopic Dermatitis. *J Allergy Clin Immunol* (2020) 145(6):1615–28. doi: 10.1016/j.jaci.2020.01.042

34. Nguyen QH, Pervolarakis N, Blake K, Ma D, Davis RT, James N, et al. Profiling Human Breast Epithelial Cells Using Single Cell RNA Sequencing Identifies Cell Diversity. *Nat Commun* (2018) 9(1):2028. doi: 10.1038/s41467-018-04334-1

35. Muhl L, Genove G, Leptidis S, Liu J, He L, Mocci G, et al. Single-Cell Analysis Uncovers Fibroblast Heterogeneity and Criteria for Fibroblast and Mural Cell Identification and Discrimination. *Nat Commun* (2020) 11(1):3953. doi: 10.1038/s41467-020-18511-8

36. Liu X, Chen W, Li W, Li Y, Priest JR, Zhou B, et al. Single-Cell RNA-Seq of the Developing Cardiac Outflow Tract Reveals Convergent Development of the Vascular Smooth Muscle Cells. *Cell Rep* (2019) 28(5):1346–61.e4. doi: 10.1016/j.celrep.2019.06.092

37. Zhao Q, Eichten A, Parveen A, Adler C, Huang Y, Wang W, et al. Single-Cell Transcriptome Analyses Reveal Endothelial Cell Heterogeneity in Tumors and Changes Following Antiangiogenic Treatment. *Cancer Res* (2018) 78 (9):2370–82. doi: 10.1158/0008-5472.CAN-17-2728

38. Shi J, Zhang L, Zhou D, Zhang J, Lin Q, Guan W, et al. Biological Function of Ribosomal Protein L10 on Cell Behavior in Human Epithelial Ovarian Cancer. *J Cancer* (2018) 9(4):745–56. doi: 10.7150/jca.21614

39. Xu H, Zhong L, Deng J, Peng J, Dan H, Zeng X, et al. High Expression of ACE2 Receptor of 2019-Ncov on the Epithelial Cells of Oral Mucosa. *Int J Oral Sci* (2020) 12(1):8. doi: 10.1038/s41368-020-0074-x

40. Lindsay J, Wang LL, Li Y, Zhou SF. Structure, Function and Polymorphism of Human Cytosolic Sulfotransferases. *Curr Drug Metab* (2008) 9(2):99–105. doi: 10.2174/138920008783571819

41. Jiang T, Chen ZH, Chen Z, Tan D. SULF2 Promotes Tumorigenesis and Inhibits Apoptosis of Cervical Cancer Cells Through the ERK/AKT Signaling Pathway. *Braz J Med Biol Res* (2020) 53(2):e8901. doi: 10.1590/1414-431x20198901

42. Walker C, Mojares E, Del Rio Hernandez A. Role of Extracellular Matrix in Development and Cancer Progression. *Int J Mol Sci* (2018) 19(10):3028–59. doi: 10.3390/ijms19103028

43. Stan RV, Kubitza M, Palade GE. PV-1 Is a Component of the Fenestral and Stomatal Diaphragms in Fenestrated Endothelia. *Proc Natl Acad Sci USA* (1999) 96(23):13203–7. doi: 10.1073/pnas.96.23.13203

44. Hamilton BJ, Tse D, Stan RV. Phorbol Esters Induce PLVAP Expression *via* VEGF and Additional Secreted Molecules in MEK1-Dependent and P38, JNK and PI3K/Akt-Independent Manner. *J Cell Mol Med* (2019) 23(2):920–33. doi: 10.1111/jcmm.13993

45. Stan RV, Tse D, Deharvengt SJ, Smits NC, Xu Y, Luciano MR, et al. The Diaphragms of Fenestrated Endothelia: Gatekeepers of Vascular Permeability and Blood Composition. *Dev Cell* (2012) 23(6):1203–18. doi: 10.1016/j.devcel.2012.11.003

46. Herrnberger L, Seitz R, Kuespert S, Bosl MR, Fuchshofer R, Tamm ER. Lack of Endothelial Diaphragms in Fenestrae and Caveolae of Mutant Plvap-Deficient Mice. *Histochem Cell Biol* (2012) 138(5):709–24. doi: 10.1007/s00418-012-0987-3

47. Wang XX, Liao Y, Hong L, Zeng Z, Yuan TB, Xia X, et al. Tissue Microarray Staining Reveals PLD1 and Sp1 Have a Collaborative, Pro-Tumoral Effect in Patients With Osteosarcomas. *Oncotarget* (2017) 8(43):74340–7. doi: 10.18632/oncotarget.20605

48. Kolanjiappan K, Manoharan S, Kayalvizhi M. Measurement of Erythrocyte Lipids, Lipid Peroxidation, Antioxidants and Osmotic Fragility in Cervical Cancer Patients. *Clin Chim Acta* (2002) 326(1-2):143–9. doi: 10.1016/S0009-8981(02)00300-5

49. Pardoll DM. The Blockade of Immune Checkpoints in Cancer Immunotherapy. *Nat Rev Cancer* (2012) 12(4):252–64. doi: 10.1038/nrc3239

50. Hannesdottir L, Tymoszuk P, Parajuli N, Wasmer MH, Philipp S, Daschil N, et al. Lapatinib and Doxorubicin Enhance the Stat1-Dependent Antitumor Immune Response. *Eur J Immunol* (2013) 43(10):2718–29. doi: 10.1002/eji.201242505

51. Zhang P, Yang M, Zhang Y, Xiao S, Lai X, Tan A, et al. Dissecting the Single-Cell Transcriptome Network Underlying Gastric Premalignant Lesions and Early Gastric Cancer. *Cell Rep* (2020) 30(12):4317. doi: 10.1016/j.celrep.2020.03.020

52. Elango R, Alsaleh KA, Vishnubalaji R, Manikandan M, Ali AM, Abd El-Aziz N, et al. MicroRNA Expression Profiling on Paired Primary and Lymph Node Metastatic Breast Cancer Revealed Distinct microRNA Profile Associated With LNM. *Front Oncol* (2020) 10:756. doi: 10.3389/fonc.2020.00756

53. Dai JB, Zhu B, Lin WJ, Gao HY, Dai H, Zheng L, et al. Identification of Prognostic Significance of BIRC5 in Breast Cancer Using Integrative Bioinformatics Analysis. *Biosci Rep* (2020) 40(2):BSR20193678. doi: 10.1042/BSR20193678

54. Baker D, Marta M, Pryce G, Giovannoni G, Schmierer K. Memory B Cells Are Major Targets for Effective Immunotherapy in Relapsing Multiple Sclerosis. *EBioMedicine* (2017) 16:41–50. doi: 10.1016/j.ebiom.2017.01.042

55. LoPiccolo J, Blumenthal GM, Bernstein WB, Dennis PA. Targeting the PI3K/Akt/mTOR Pathway: Effective Combinations and Clinical Considerations. *Drug Resist Updat* (2008) 11(1-2):32–50. doi: 10.1016/j.drup.2007.11.003

56. Cassinelli G, Zuco V, Gatti L, Lanzi C, Zaffaroni N, Colombo D, et al. Targeting the Akt Kinase to Modulate Survival, Invasiveness and Drug Resistance of Cancer Cells. *Curr Med Chem* (2013) 20(15):1923–45. doi: 10.2174/09298673113209990106

57. Steelman LS, Navolanic P, Chappell WH, Abrams SL, Wong EW, Martelli AM, et al. Involvement of Akt and mTOR in Chemotherapeutic- and Hormonal-Based Drug Resistance and Response to Radiation in Breast Cancer Cells. *Cell Cycle* (2011) 10(17):3003–15. doi: 10.4161/cc.10.17.17119

58. Achkar IW, Abdulrahman N, Al-Sulaiti H, Joseph JM, Uddin S, Mraiche F. Cisplatin Based Therapy: The Role of the Mitogen Activated Protein Kinase Signaling Pathway. *J Transl Med* (2018) 16(1):96. doi: 10.1186/s12967-018-1471-1

59. Kawano M, Mabuchi S, Matsumoto Y, Sasano T, Takahashi R, Kuroda H, et al. The Significance of G-CSF Expression and Myeloid-Derived Suppressor Cells in the Chemoresistance of Uterine Cervical Cancer. *Sci Rep* (2015) 5:18217. doi: 10.1038/srep18217

60. Li C, Guo L, Li S, Hua K. Single-Cell Transcriptomics Reveals the Landscape of Intra-Tumoral Heterogeneity and Transcriptional Activities of ECs in CC. *Mol Ther Nucleic Acids* (2021) 24:682–94. doi: 10.1016/j.omtn.2021.03.017

61. Paraiso KH, Smalley KS. Fibroblast-Mediated Drug Resistance in Cancer. *Biochem Pharmacol* (2013) 85(8):1033–41. doi: 10.1016/j.bcp.2013.01.018

62. Erez N, Glanz S, Raz Y, Avivi C, Barshack I. Cancer Associated Fibroblasts Express Pro-Inflammatory Factors in Human Breast and Ovarian Tumors. *Biochem Biophys Res Commun* (2013) 437(3):397–402. doi: 10.1016/j.bbrc.2013.06.089

63. Fukumura D, Xavier R, Sugiura T, Chen Y, Park EC, Lu N, et al. Tumor Induction of VEGF Promoter Activity in Stromal Cells. *Cell* (1998) 94(6):715–25. doi: 10.1016/S0092-8674(00)81731-6

64. Logan CY, Nusse R. The Wnt Signaling Pathway in Development and Disease. *Annu Rev Cell Dev Biol* (2004) 20:781–810. doi: 10.1146/annurev.cellbio.20.010403.113126

65. Clevers H. Wnt/beta-Catenin Signaling in Development and Disease. *Cell* (2006) 127(3):469–80. doi: 10.1016/j.cell.2006.10.018

66. Zhou Y, Huang Y, Cao X, Xu J, Zhang L, Wang J, et al. WNT2 Promotes Cervical Carcinoma Metastasis and Induction of Epithelial-Mesenchymal Transition. *PLoS One* (2016) 11(8):e0160414. doi: 10.1371/journal.pone.0160414

67. Sontake V, Wang Y, Kasam RK, Sinner D, Reddy GB, Naren AP, et al. Hsp90 Regulation of Fibroblast Activation in Pulmonary Fibrosis. *JCI Insight* (2017) 2(4):e91454. doi: 10.1172/jci.insight.91454

68. Turley SJ, Cremasco V, Astarita JL. Immunological Hallmarks of Stromal Cells in the Tumour Microenvironment. *Nat Rev Immunol* (2015) 15(11):669–82. doi: 10.1038/nri3902

69. Talmadge JE, Gabrilovich DI. History of Myeloid-Derived Suppressor Cells. *Nat Rev Cancer* (2013) 13(10):739–52. doi: 10.1038/nrc3581

70. Rodig N, Ryan T, Allen JA, Pang H, Grabie N, Chernova T, et al. Endothelial Expression of PD-L1 and PD-L2 Down-Regulates CD8+ T Cell Activation and Cytolysis. *Eur J Immunol* (2003) 33(11):3117–26. doi: 10.1002/eji.200324270

71. Wendel Naumann R, Leath CA3rd. Advances in Immunotherapy for Cervical Cancer. *Curr Opin Oncol* (2020) 32(5):481–7. doi: 10.1097/CCO.0000000000000663

72. Kim D, Dan HC, Park S, Yang L, Liu Q, Kaneko S, et al. AKT/PKB Signaling Mechanisms in Cancer and Chemoresistance. *Front Biosci* (2005) 10:975–87. doi: 10.2741/1592

73. Brognard J, Clark AS, Ni Y, Dennis PA. Akt/protein Kinase B Is Constitutively Active in Non-Small Cell Lung Cancer Cells and Promotes Cellular Survival and Resistance to Chemotherapy and Radiation. *Cancer Res* (2001) 61(10):3986–97.